JOURNAL OF GEOPHYSICAL RESEARCH, VOL. 99, NO. A9, PAGES 17,511–17,522, SEPTEMBER 1, 1994

Simultaneous observations of VLF ground transmitter signals on the DE 1 and COSMOS 1809 satellites: Detection of a magnetospheric caustic and a duct

V. S. Sonwalkar, U. S. Inan, T. F. Bell, and R. A. Helliwell

Space, Telecommunications, and Radioscience Laboratory, Stanford University, Stanford, California

V. M. Chmyrev, Ya. P. Sobolev, O. Ya. Ovcharenko, and V. Selegej

Institute of Terrestrial Magnetism, Ionosphere and Radiowave Propagation, USSR Academy of Sciences, Troitsk, Moscow Region, Russia

Abstract. Khabarovsk transmitter signals (15.0 kHz, 48°N, 135°E) were observed on the high-altitude (~15000 km) Dynamic Explorer 1 (DE 1) and the low-altitude (~960) km COSMOS 1809 satellites during a 9-day period in August 1989. On 7 out of 9 days the linear wave receiver (LWR) on the DE 1 satellite detected signals from the Khabarovsk transmitter. In addition, the DE 1 satellite also detected signals from the Alpha transmitter (11.9-15.6 kHz) in Russia and an Omega transmitter (10.2-13.6 kHz) in Australia, as well as natural VLF emissions such as hiss, chorus, whistlers, and wideband impulsive signals. On two days, August 23 and 27, 1989, observations of the Khabarovsk transmitter signals were simultaneously carried out at high altitude on the DE 1 satellite and at low altitude on the COSMOS 1809 satellite. Analysis of data from these 2 days has led to several new results on the propagation of whistler mode signals in the Earth's magnetosphere. New evidence was found of previously reported propagation phenomena, such as (1) confinement of transmitter signals in the conjugate hemisphere at ionospheric heights (~1000 km), (2) observation of direct multipath propagation on both DE 1 and COSMOS 1809, (3) detection of ionospheric irregularities of $\leq$ 100 km scale size with a few percent enhancement in electron density, believed to be responsible for the observed multipath propagation. We report the first detection of an exterior caustic surface near $L \sim 3.5$ for VLF ground transmitter signals injected into the magnetosphere; the location of the caustic surface depended on the signal frequency, and the electric and magnetic fields decreased by several hundred decibels per L shell in the dark (shadow) side of the caustic. We also report the first direct detection of a magnetospheric duct at $L = 2.94$ which was believed to be responsible for the ducted propagation of Khabarovsk signals observed on the COSMOS 1809 satellite; the measured duct parameters were: $\Delta L \sim 0.06$ and $\Delta N_e \sim 10 - 13\%$. The duct width at the equator was ~367 km. Our study also indicates that duct end points can extend down to at least ~1000 km. The peak electric and magnetic fields of ducted Khabarovsk transmitter signals at ~1000 km were 520 μV/m and 36 pT respectively. Estimated field strengths of these signals inside the duct at the geomagnetic equator were 57 μV/m and 12 pT for electric and magnetic field respectively. The results of two-dimensional ray tracing simulations were consistent with the observations of the nonducted whistler-mode propagation of Khabarovsk (15 kHz) and Alpha (11.9 kHz) signals from the transmitter location to the DE 1 and COSMOS 1809 satellites. Our results have direct implications for the question of accessibility of waves injected from the ground to various regions of the ionosphere and the magnetosphere. In situ measurements of electric and magnetic fields of Khabarovsk transmitter signals inside a duct may well prove to be the critical measurements needed to differentiate between the small signal and large signal theories of wave particle interactions.

Introduction

Previous satellite observations have shown that a major fraction of the VLF/ELF energy introduced into the magnetosphere from the ground by lightning and manmade signals propagates in the nonducted mode with wave normals that make large angles with respect to the geomagnetic field [*Edgar*, 1976; *Bell et al.*, 1981; *Neubert et al.*, 1983; *Sonwalkar and Inan*, 1986; *Draganov et al.*, 1993]. An increasing amount of evidence also suggests that nonducted waves, propagating obliquely to the geomagnetic field, can play a significant role in magnetospheric wave particle interactions. Ground transmitter signals propagating with large wave normal angles have been found to trigger VLF emissions [*Bell et al.*, 1981]. In the presence of plasma density irregularities, ground transmitter signals and whistlers can generate lower hybrid waves, which in turn can lead to ion heating [*Bell and Ngo*, 1988; *Bell et al.*, 1991]. Magnetospherically reflected (MR) whistlers, propagating at angles close to the whistler mode res-

Paper number 94JA00866.
0148-0227/94/94JA-00866$05.00

onance cone, can precipitate electrons in the few hundred eV energy range [*Jasna et al.*, 1990, 1992]. Natural signals such as plasmaspheric and auroral hiss, believed to originate in the magnetosphere, have also been found to propagate at large wave normal angles [*Maggs*, 1976; *Gurnett et al.*, 1983; *Lefeuvre et al.*, 1983; *Hayakawa et al.*, 1986; *Sonwalkar and Inan*, 1988; *Storey et al.*, 1991; *Draganov et al.*, 1993]. MR whistlers have been found to generate hisslike emissions, also propagating at large wave normal angles [*Sonwalkar and Inan*, 1989; *Draganov et al.*, 1992, 1993].

Waves propagating with wave normals approximately aligned with the Earth's magnetic field are believed to propagate in field-aligned ducts of enhanced or depressed ionization [*Smith et al.*, 1960; *Helliwell*, 1965]. These ducted waves are rarely observed on satellites in the magnetosphere due to the relatively small volume (0.01%) apparently occupied by the ducts [*Burgess and Inan*, 1993] but are most commonly observed on the ground after they have exited from a duct and propagated in the Earth-ionosphere wavguide to a receiving site [*Helliwell*, 1965]. Ground transmitter signals, whistlers, and chorus propagating in the ducted mode have been found to trigger VLF emissions of various kinds [*Helliwell*, 1965, 1988] and to precipitate energetic electrons [*Rosenberg et al.*, 1971; *Helliwell et al.*, 1973; *Voss et al.*, 1984; *Inan et al.*, 1990]. Detailed measurements of the properties of ducts (size and enhancements) and of ducted waves are important to properly evaluate various theories of wave particle interactions and to determine the extent of the particle precipitation due to ducted waves [*Helliwell*, 1988; *Burgess and Inan*, 1993]. While the duct hypothesis has been extensively used in interpreting ground observations of VLF waves, only a limited set of experimental data is available that provides for the determination of properties of magnetospheric ducts based on in situ observations [*Smith and Angerami*, 1968; *Angerami*, 1970; *Scarf and Chappell*, 1973; *Carpenter et al.*, 1981; *Koons*, 1989].

The study of ducted and nonducted modes of wave propagation is an important area of magnetospheric physics. While a large number of investigations have been conducted on this subject in the past, a collaborative study between Stanford (California) and IZMIRAN (Russia) conducted in August 1989 has produced a unique set of data showing new aspects of the propagation of ground transmitter signals in the Earth's magnetosphere. The uniqueness of the data set lies in the fact that simultaneous measurements of signals from a very powerful ground transmitter were performed on the ionospheric satellite COSMOS 1809 and the magnetospheric satellite DE 1, and that both nonducted and ducted modes of propagation were observed. We present the first measurements of the intensity of electric and magnetic fields as the DE 1 satellite trajectory crossed an exterior caustic surface in the magnetosphere. We also present direct evidence for the in situ detection of a magnetospheric duct and measurements of the intensities of both electric and magnetic fields of ground transmitter signals inside a duct. The observations are interpreted with the help of ray tracing simulations. The implications of our results for magnetospheric wave particle interactions are discussed.

Experiment Description

The VLF transmitter at Khabarovsk, Russia (48°N, 135°E; $\lambda_m \sim 38°, \phi_m \sim -158°$) was used to inject waves into the magnetosphere in August 1989. The transmitter operated at 15.0 kHz in a 4 s On/4 s Off transmission mode, radiating ~800-kW power. The electric and magnetic fields of the injected waves were recorded by VLF receivers on the COSMOS 1809 and DE 1 satellites. In addition to the Khabarovsk transmitter, signals from the Alpha transmitter (11.9-15.6 kHz, 50.5°N, 137°E, 10-500 kW) at Komsomolskamur in Russia and the Omega transmitter (10.2-13.6 kHz, 36°S, 150°E, 10 kW) in Australia, as well as natural VLF wave activity, were also observed. In addition to making wave measurements, the COSMOS 1809 satellite was equipped to measure electron density with high temporal resolution.

COSMOS 1809 was in a near-circular orbit at an altitude of ~960 km and inclination of ~82.5°. ELF/VLF measurements were made with a five-channel spectrum analyzer with electric (E_y) and magnetic (B_x) antennas measuring fields in a horizontal plane along the northsouth and east-west directions, respectively. The central frequencies of the analyzer were 140, 450, 800, 4500, and 15000 Hz, and the channel bandwidths were 16.67% of the channel central frequencies. The data were sampled once every 320 ms.

The DE 1 satellite was in a polar orbit with perigee at ~ 520 km and apogee at 4.66 R_E. The altitude of the satellite when the Khabarovsk signals were received was ~15,000 km. The DE 1 data utilized in this paper were acquired using the linear wave receiver (LWR), which was integrated into the plasma wave instrument (PWI) [*Shawhan et al.*, 1981] and measures wave amplitudes in three frequency bands: 1.5–3.0 kHz, 3.0–6.0 kHz, and 10.0–16.0 kHz. The gain of the amplifier could be set at 10-dB steps over a 70-dB range and could be varied automatically or commanded to remain fixed at any level. The response was linear over a 30-dB range in any gain position, thus facilitating accurate measurement of signal intensity and temporal growth rate. The LWR could be commanded to cycle between a 200-m-long electric dipole and a 0.8-m by 1.25-m single-turn loop magnetic antenna. The receiver allowed for detailed quantitative study of phenomena within the passband, providing for measurement of signal growth characteristics as well as spin fading [*Rastani et al.*, 1985; *Sonwalkar and Inan*, 1986]. The antennas on DE 1 could also be connected to a wideband receiver (WBR) with an automatic gain control (AGC) amplifier. The WBR had a dynamic range of 100 dB and covered a wide frequency range [*Shawhan et al.*, 1981]. The results presented here are based on the data received by the LWR operating in the 10 - 16 kHz band and toggled between the 200-m-long electric dipole and 1 m^2 magnetic loop every 30 s, thus giving nearly simultaneous measurements of electric and magnetic fields.

Observations and Interpretations

Table 1 summarizes the circumstances of the experiment and the DE 1 observations of VLF waves in the 10-16 kHz band. The Khabarovsk transmitter was operated on nine days between August 7 and 27, 1989. The DE 1 orbit parameters were approximately the same for these days during the transmission period, with DE 1 at 13,000 km altitude and 8°N geomagnetic latitude at the beginning of the transmission and at 18,000 km altitude and 5°S at the end of the transmission. The geographic longitude of the satellite was ~115°E. Figure 1 shows the DE 1 trajectory during the observation period on August 23, 1989, representative also of the DE 1 orbits on other days listed in Table 1.

Signals from the Khabarovsk, Russia (15.0 kHz), Alpha, Russia (11.905, 12.5, 12.649, 13.281, 14.881, 15.625 kHz), and Omega, Australia (10.2, 11.05, 11.33, 13.0, 13.6 kHz) transmitters were observed on several days. Natural VLF waves such as whistlers, hiss, chorus, and wideband impulses were also observed. As shown in the Table 1, the Khabarovsk signal was detected on the

Table 1. Summary of the DE 1-Khabarovsk Experiments (August 1-29, 1989)

Day	DE 1 Recordings	Khabarovsk(KH) Transmissions	Comments (Signals Seen)	KPMAX
Aug. 7	1655-1725	1630-1730	KH, Alpha, Omega Whistler, Hiss	3+
Aug. 9	1655-1725	1630-1730	KH, Alpha, Omega Whistler, Hiss	2-
Aug. 13	1637-1707	1610-1710	KH, Alpha, Omega Whistler, Hiss	3
Aug. 15	1625-1655	1555-1655	KH, Alpha, Omega Whistler, Hiss	7-
Aug. 17	1620-1650	1550-1650	Impulsive noise Discrete chorus elements	5
Aug. 19	1612-1642	1600-1700	KH, Alpha, Omega Whistler, Hiss	5
Aug. 21	1607-1637	1610-1710	Impulsive noise Discrete chorus elements	3
Aug. 23	1554-1624	1540-1640	KH, Alpha, Omega Impulsive noise, Chorus	5
Aug. 27	1543-1613	1520-1620	KH, Alpha, Omega Whistler, Hiss	4

DE 1 satellite on 7 out of the 9 days. Absence of any transmitter signals on August 17 and 21, 1989 was probably due to DE 1 being outside the plasmasphere as indicated by the presence of chorus and impulsive wideband noise, and the absence of plasmaspheric hiss [*Thorne et al.*, 1973; *Burtis and Helliwell*, 1976; *Ondoh et al.*, 1989; *Sonwalkar et al.*, 1990].

We now present a detailed report on the case of August 23, 1989 when simultaneous observations of Khabarovsk (Kh) transmitter signals were made on the COSMOS 1809 and DE 1 satellites. Because of the wide bandwidth of LWR, DE 1 also recorded signals from the Alpha and Omega transmitters. Similar observations were made on August 27, 1989.

Figures 1a and 1b display the DE 1 and COSMOS 1809 satellite orbits in the magnetic meridional and magnetic equatorial planes respectively when Khabarovsk signals were observed on the two satellites on August 23, 1989. Figure 2 shows a wide band spectrum (10-16 kHz) of VLF signals recorded by the LWR on August 23, 1989. Khabarovsk, Alpha, and Omega transmitter signals, as well as whistlers (vertical traces), are clearly visible in the spectrum. Figure 3a shows COSMOS 1809 observations of Khabarovsk signals in the 15-kHz channel of the spectrum analyzer when the satellite passed over the transmitter at ~1600 UT and when the satellite passed over a region roughly magnetically conjugate to the transmitter location in the southern hemisphere at ~1622 UT. Figure 3 presents electric field E_y, magnetic field B_x, mean square root variation in the electron density dN_e, and the total electron density N_e along the satellite orbit. Since the satellite altitude during this interval was approximately constant, dN_e is a measure of horizontal gradients in the ionospheric electron density. Figures 3b, 3c, and 3d reproduce in detail parts of figure 3a when strong Khabarovsk signals were observed on the COSMOS 1809 satellite in the northern and the southern hemispheres. The measured time delays of the Khabarovsk signals for propagation to the DE 1 satellite were ~1.2-1.3 s.

Salient features of our observations of transmitter signals on the two satellites and their interpretations in terms of ducted and nonducted whistler mode propagation are described below.

Observations of Transmitter Signals Over the Transmitter and Their Confinement in the Conjugate Hemisphere

As seen in Figure 3a, transmitter signals were observed in the northern hemisphere when the COSMOS 1809 satellite passed over the transmitter location and also in the southern hemisphere in a region approximately magnetically conjugate to the trans-

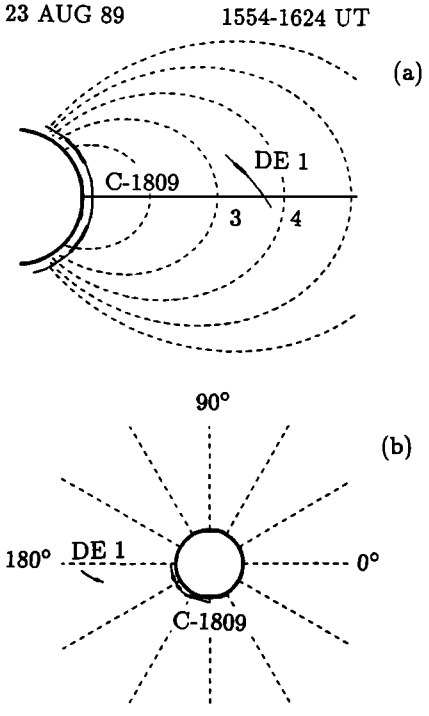

Figure 1. Orbits of DE 1 and COSMOS 1809 satellites in magnetic meridional and equatorial planes on August 23, 1989 during the period when the Khabarovsk transmitter was operating. The thickened parts of the orbits indicate the time period during which the transmitter signals were detected on the satellites.

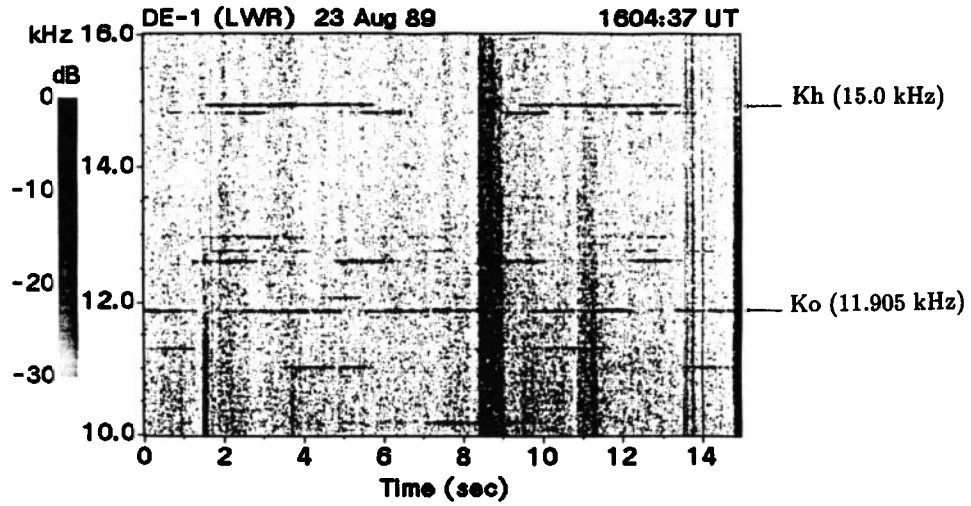

Figure 2. An example of a spectrum showing reception of various ground transmitter signals on the DE 1 satellite. The arrows point to 15.0- and 11.9-kHz signals from transmitters at Khabarovsk (Kh) and at Komsomolskamur (Ko), respectively.

mitter. Since the satellite altitude was well above the D region, these signals were observed after passing through the region of absorption in the D layer in the northern hemisphere. Figures 3b, 3c, and 3d in which individual 4-s-long transmitter pulses can be seen, give a detailed plot of the electric and magnetic fields measured in these two regions. The electric field detector recorded pulses over larger regions compared to the magnetic field detector due to the higher sensitivity of the former. Table 2 gives the parameters of the regions in the two hemispheres where nonducted and ducted (indicated in Figure 3a) Khabarovsk signals were detected by the COSMOS 1809 satellite. The propagation in the northern hemisphere was assumed to be nonducted, though wave normal angles near the transmitter latitude are typically small due to the nearly vertical propagation that waves undergo after entering the ionosphere from below. The beginning and end times are indicated when the signal fell below 10% ($\leq$ 50 μV/m) of the peak value ($\sim$ 520 μV/m) of the electric field. The L shell ranges over which nonducted signals were observed were 1.4 to 3.0 and 1.35 to 3.4 for the northern and southern hemispheres respectively. This observed confinement of nonducted waves in the conjugate hemisphere is consistent with previous OGO 4 (altitude $\sim$ 400 – 900 km) observations of NAA transmitter signals (17.8 kHz) [*Scarabucci*, 1969] and FR 1 (altitude $\sim$750 km) observations of FUB transmitter signals (16.8 kHz) [*Cerisier*, 1973]. Assuming that the propagation takes place in the magnetic meridional plane, our observations indicate that the longitude range over which detectable signals are observed in both hemispheres is $\pm 11^{\circ}$ centered on the longitude of the transmitter.

As indicated in Figures 3a and 3d, and in the third major column of Table 2, signals detected at 1625 UT in the southern hemisphere with a relatively large magnetic field component are interpreted as having propagated in the ducted mode. These are discussed further in subsection 3.5.

Direct Multipath Propagation: Detection of 10-100 km Scale Electron Density Irregularities in the Ionosphere

It has been noted previously that direct multiple path propagation is a common feature of the waves injected from the ground and observed in the magnetosphere [*Sonwalkar et al.*, 1984]. In this kind of propagation, signals from a subionospheric source reach a satellite via several different propagation paths leading to amplitude modulation and pulse elongation of the observed signals. This effect, attributed to the presence of horizontal density gradients in the ionosphere, was observed for the transmitter pulses observed on DE 1 for all seven days. On August 23, 1989, the Khabarovsk transmitter pulses were stretched by $\sim$300 ms as a result of multipath propagation. The pulse amplitude exhibited modulation at frequencies other than the spin frequency, thus confirming the presence of multipath.

Simultaneous observations of VLF waves and electron density on COSMOS 1809 provides a unique opportunity to measure the parameters of density irregularities responsible for direct multiple path propagation. The top two panels of Figures 3a, 3b, and 3c show the amplitude fading of Khabarovsk transmitter signals due to multiple path propagation effects and the third panel shows the fluctuations ΔN_e in the electron density believed to be responsible for the multiple path propagation. The typical horizontal extent of these irregularities was $\leq$100 km and the density fluctuations were of the order of $\leq$5%, consistent with previous theoretical estimates obtained using wave observations and ray tracing simulations [*Sonwalkar et al.*, 1984].

Detection of Magnetospheric Caustic Surfaces: A Frequency-Dependent Spatial Cutoff of the Nonducted Ground Transmitter Signals Observed on the DE 1 Satellite

DE 1 observations of the Khabarovsk and Alpha ground transmitter signals revealed a frequency dependent spatial cutoff for nonducted waves. For the discussion presented here these two transmitters, which are within $\sim$310 km of each other, can be assumed to be located at the same place. Figures 4a and 4b show the electric and magnetic field intensity of Alpha (11.9) and Khabarovsk (15.0 kHz) signals respectively for August 23, 1989, and Figures 5a and 5b show the same for August 27, 1989. The main features of this cutoff as listed in Table 3 are the following:

1. The higher frequencies cutoff at lower L shells.
2. Close to the cutoff, electric and magnetic fields decrease exponentially with typical rates of several hundred decibels per unit L shell. The rate of the decrease is higher for higher frequencies and is higher for the electric field compared to that for the magnetic field.
3. Just before the fields begin to decrease, they show an enhancement in amplitude. This feature is evident in Figure 5 but not so pronounced in Figure 4.

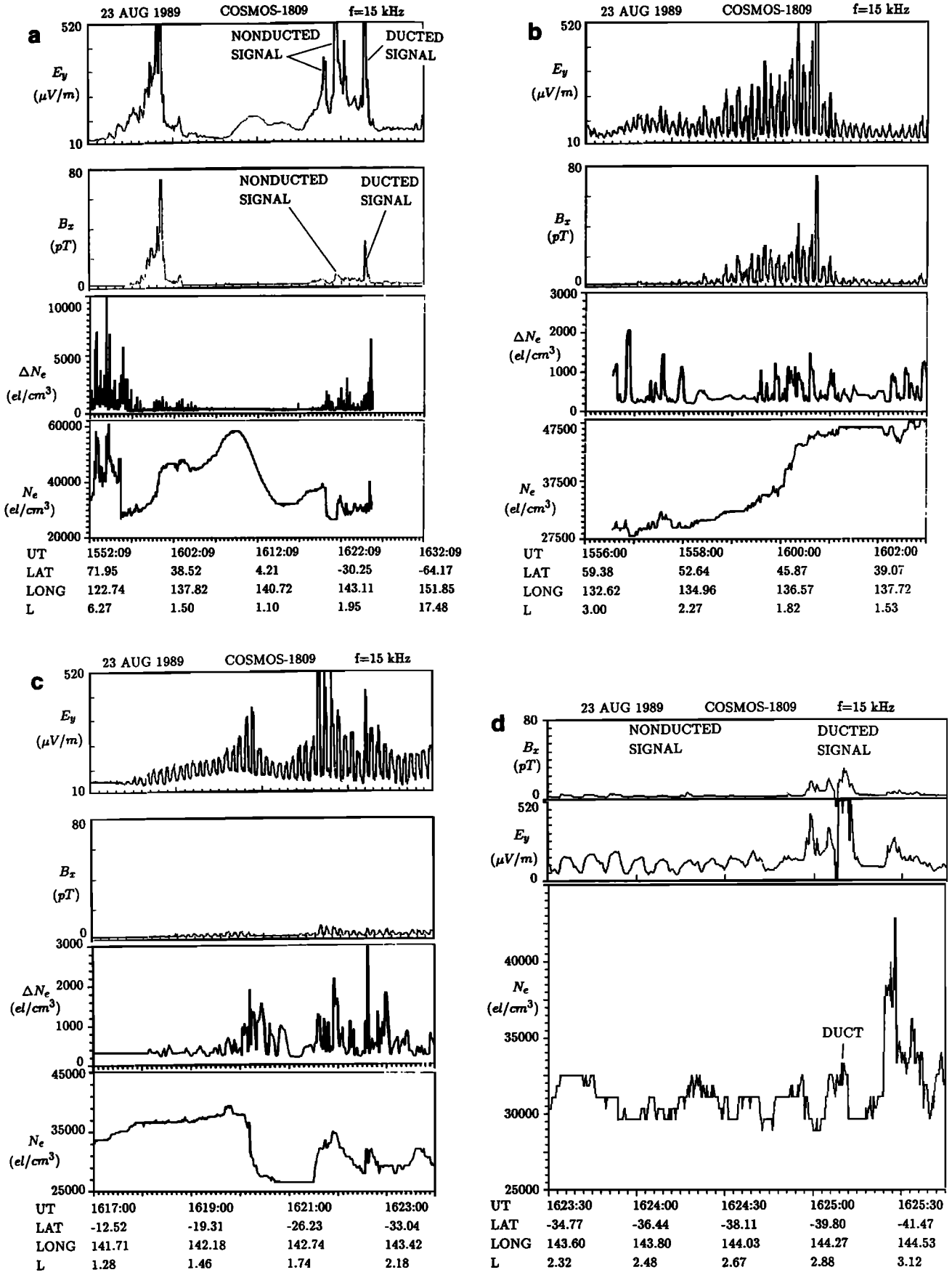

Figure 3. (a) Amplitude of electric and magnetic fields of Kh signals on COSMOS 1809 satellites for August 23, 1989. Also shown are the mean square root variation in the electron density dN_e and electron density (Ne). (b) and (c) Close relations between the amplitude modulation resulting from the mulitple path propagation and the kilometer scale electron density irregularities responsible for them. (d) The signal propagating in the ducted mode and the cross section of the duct as observed on the COSMOS 1809 satellite. The sharp decrease in the electric and magnetic fields at 1625:06 for $\sim$ 1 s is the result of telemetry failure.

Table 2. Parameters of Nonducted and Ducted Propagation Observed on the COSMOS 1809 Satellite

	Northern Hemisphere Nonducted Propagation		Southern Hemisphere Nonducted Propagation		Southern Hemisphere Ducted Propagation	
	Begin	End	Begin	End	Begin	End
UT	1556	1603	1618	1626	1624:57	1625:15
ALT	958.6	957.9	969.3	982.5	980.9	981.05
LAT	59.4°	35.7°	−15.9°	−43.2°	−39.627°	−40.581°
LONG	132.6°	138.2°	141.9°	144.8°	144.246°	144.387°
INV LAT	52.4°	27.9°	26.33°	55.1°	51.516°	52.505°
L	3.0	1.4	1.35	3.4	2.859	2.987
Peak E_y	> 520μV/m		> 520μV/m		> 520μV/m	
Peak B_x	75 pT		8 pT		36 pT	
$(CB_x/E_y)^*_{\text{average}}$	~20-25		~2-5		~17-19	

*In calculating $(CB_x/E_y)_{\text{average}}$ ratio, pulses for which the electric field intensity exceeded the instrument upper limit of 520 μV/m were not included.

We interpret this cutoff as the detection of an exterior magnetospheric caustic for nonducted waves injected from the ground. A surface forming the envelope of a system of rays is called a caustic surface. Figures 8a and 8b show examples of exterior caustics for 11.9- and 15.0-kHz transmitter signals propagating in the magnetosphere, as determined from raytracing. The features shown here are called exterior caustics because they are outer boundaries of the regions where the propagation takes place. The region inside the caustic, accesssible to rays, is called the illuminated side of the caustic and the region outside, the dark or shadowed side of the caustic. While the theory of caustic surfaces for anisotropic magnetoplasmas has not yet been fully developed, an approxi-

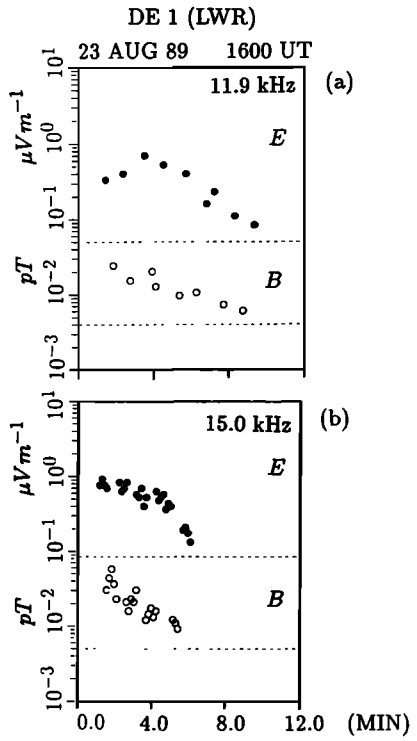

λ_m	8.3°N	2.5°N
L	3.38	3.57
ϕ_g	118.4	115.5
ALT(km)	14660	16331

Figure 4. (a) Amplitudes of electric and magnetic fields of 11.9-kHz Alpha transmitter signals observed on DE 1 on August 23, 1989. (b) Amplitudes of electric and magnetic fields of 15.0-kHz Khabarovsk transmitter signals observed on DE 1 on August 23, 1989.

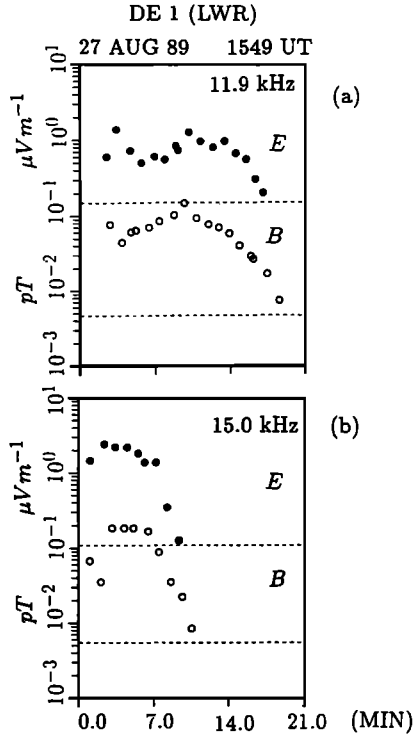

λ_m	7.1°N	2.0°S
L	3.47	3.84
ϕ_g	117.2	112.0
ALT(km)	15376	18005

Figure 5. (a) Amplitudes of electric and magnetic fields of 11.9-kHz Alpha transmitter signals observed on DE 1 on August 27, 1989. (b) Amplitudes of electric and magnetic fields of 15.0-kHz Khabarovsk transmitter signals observed on DE 1 on August 27, 1989.

Table 3. Signal Characteristics in the Dark Side of the Caustic

	August 23, 1989				August 27, 1989			
	11.9kHz		15.0kHz		11.9kHz		15.0kHz	
	E	*B*	*E*	*B*	*E*	*B*	*E*	*B*
Background noise level*	0.05 μV/m	0.004 pT	0.085 μV/m	0.005 pT	0.15 μV/m	0.005 pT	0.1μV/m	0.005pT
Rate of decrease of field in dB per L-shell	187	118	561	496	249	196	502	382
L shell value when the signal intensity falls below the background noise level†	3.56	3.56	3.48	<3.48	<3.77	3.77	<3.58	3.58

* A 100-Hz filter was used.

† larger of the values found for E or B are given.

mate full wave treatment indicates that the signal intensity near a caustic is given by an Airy integral function [*Budden*, 1985]. Though there are no real rays outside the caustic (dark side), the signal does not fall abruptly to zero, but decays rapidly. The typical features of the electric and magnetic field variations noted above, a slight increase in the intensities followed by a rapid decay, are consistent with those expected from the theory of caustics [*Budden*, 1985]. Ray tracing simulations presented in the next section indicate that the wave normal direction near the caustic surface was within 1°-2° of the whistler mode resonance cone. We believe this is the first detection of an exterior caustic with detailed electric and magnetic field intensity measurements in the high-altitude magnetosphere for nonducted VLF waves. The only previous measurements of this kind for VLF waves were reported by *Dantas* [1972] on the low-altitude (~750 km) OGO 4 satellite. He presented observations of the electric field of NAA transmitter signals at 17.80 and 17.85 kHz near an interior caustic in the ionosphere. Though the temporal (~1 s) and the length scales (~8 km) over which the intensity fell below the noise level differed from those of the data presented in this case, the electric field intensity displayed features similar to those reported above. Finally, we note that there is another kind of spatial cutoff (caustic) possible for signals injected from the ground [*Dunckel and Helliwell*, 1977]. This cutoff is observed on a satellite when the signal frequency approaches the local gyrofrequency ($f/f_H \sim 0.9$). At such locations the rays bend inward and thus become inaccessible to the satellite (see Figure 8).

Measurement of Wave Normal Direction

Simultaneous measurement on the COSMOS 1809 satellite of the electric field (E_y), magnetic field (B_x), and electron density (N_e), coupled with attitude information allow the determination of average wave normal direction [*Sonwalkar*, 1986]. Assuming whistler mode propagation in the magnetic meridional plane, the ratio $(cB_x)/E_y$ can be calculated as a function of wave normal direction θ. A comparison of the calculated ratio with the measured value leads to the determination of the wave normal direction. The assumption of whistler-mode propagation is justified because for 15-kHz signal frequency and for the plasma density and geomagnetic field values at the altitudes of the COSMOS 1809 and DE 1 satellites, this is the only allowed cold plasma propagation mode. The assumption about propagation in the magnetic meridional plane is justified based on previous wave normal direction measurements of ground transmitter signals in the magnetosphere [*Neubert et al.*, 1983; *Sonwalkar and Inan*, 1986]. Assuming a right-handed coordinate system with the z axis along the geomagnetic field and the x axis in the magnetic meridional plane, the following equation holds for a plane wave propagating in the whistler mode in the Earth's magnetosphere [*Sonwalkar*, 1986].

$$\frac{cB_{x'}}{E_{y'}} = \mu(\theta,\phi,\omega)\frac{[\mathbf{u}(\theta,\phi,\omega)\times\mathbf{R}^e(\theta,\phi,\omega)\cdot\mathbf{l}_{x'}]}{\mathbf{R}^e(\theta,\phi,\omega)\cdot\mathbf{l}_{y'}} \quad (1)$$

where $B_{x'}$ and $E_{y'}$ are the magnetic and electric field components along the directions x' and y', respectively. The quantities μ and $\mathbf{R}^e$ are, respectively, the whistler mode refractive index and electric field polarization vector for a plane wave propagating in the direction $\mathbf{u}(\theta,\phi)$, where θ and ϕ are the polar and azimuthal angles in the (x,y,z) frame. Unit vectors $\mathbf{l}_{x'}$ and $\mathbf{l}_{y'}$ are in the directions x' and y', respectively. We note here that directions x' and y' are not necessarily orthogonal.

For known values of geomagnetic field $\mathbf{B}_0$ and electron density N_e, μ and $\mathbf{R}^e$ are known functions of wave normal direction $\mathbf{u}(\theta,\phi)$. Thus, assuming propagation in the magnetic meridional plane, the ratio on the right side of (1) can be calculated as a function of wave normal direction with respect to the geomagnetic field, and comparing this with the measured ratio on the left, the wave normal direction θ can be estimated.

The measurement of the wave normal direction of the Khabarovsk signal on DE 1 employs the same method except that in situ electron density is not available, and only near simultaneous measurements of electric and magnetic field are obtained. These are not severe limitations, because the ratio of electric and magnetic field is rather insensitive to local plasma density and therefore plasma density deduced from the ray tracing plasma model (section 4) can be used. Near-simultaneous measurements of electric and magnetic field are available within 30 s. At high altitudes the location of DE 1 satellite does not vary appreciably in 30 s, and thus the wave normal directions of waves arriving from distant sources can be determined using near simultaneous values of electric and magnetic field [*Sonwalkar and Inan*, 1986].

Figure 6 shows the theoretically predicted $(cB_x)/E_y$ ratio for the typical plasma parameters along the COSMOS 1809 trajectory in the northern and southern hemisphere and for typical plasma parameters at the DE 1 location. As Figure 6 shows, at low

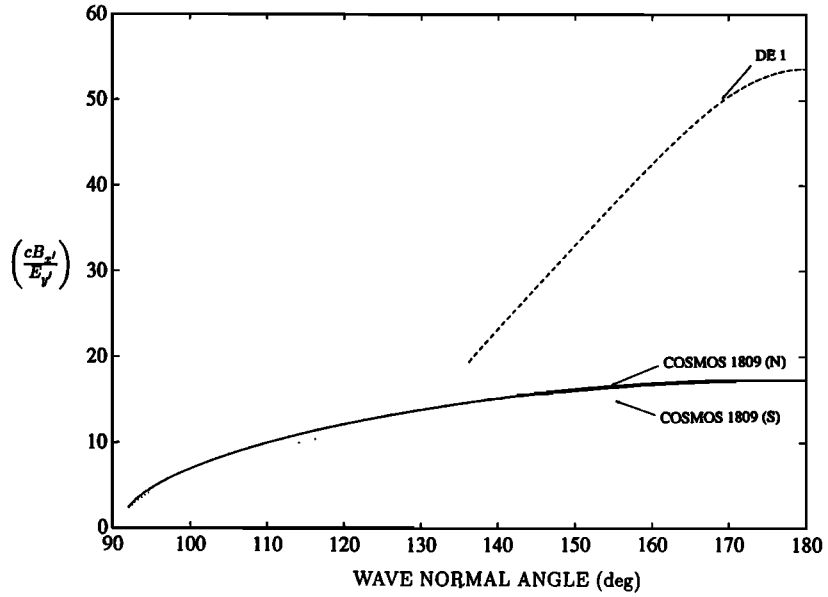

Figure 6. Theoretically predicted $(cB_x)/E_y$ ratios for typical plasma parameters along COSMOS 1809 trajectories in the northern (N_e = 37,000 electrons/cm) and southern (N_e = 35,000 electrons/cm) hemispheres and for typical plasma parameters at the DE 1 location (N_e = 6000 electrons/cm^3).

altitude (COSMOS 1809 altitudes) the ratio remains relatively constant (15-18) for wave normal angles close to $\mathbf{B}_0$ (< 150 – 180°) and falls to small values (< 5) for large ~ 90° wave normal directions (a wave propagating along the magnetic field line has wave normal angle of 180° because the geomagnetic field is pointed downward in the northern hemisphere, and the waves from the transmitter propagate upward). From Table 2 we note that the $(cB_x)/E_y$ ratio of the nonducted signals measured in the northern hemisphere is typically 20-25 and that measured in the southern hemisphere is 2-5, a factor of 5-10 smaller. At ~1625 UT a relatively large $(cB_x)/E_y$ ratio (17-19) was measured in the southern hemisphere. This has been interpreted as evidence of a ducted signal and is discussed in detail in the next subsection. Comparing the theoretical curves (assuming the peak value of $(cB_x)/E_y$ ratio from theoretical curves to be normalized to 25) for $(cB_x)/E_y$ ratio with the measured values, we conclude:

1. Wave normal directions of Khabarovsk signals observed on COSMOS 1809 in the northern hemisphere are within 20-30° of the magnetic field (neglecting the 180° factor).

2. Wave normal directions of the Khabarovsk signals observed on COSMOS 1809 in the southern hemisphere and indicated as nonducted waves in Figures 3a and 3d are close to ~ 90° with respect to the direction of the geomagnetic field.

3. Wave normal directions of the Khabarovsk signals observed on COSMOS 1809 in the southern hemisphere at 1625 UT and indicated as ducted waves in Figures 3a and 3d are within 20-30° of the magnetic field.

4. For the parameters of the DE 1 satellite the $(cB_x)/E_y$ ratio is ~ 55 for wave normal angles close to $\mathbf{B}_0$ (~ 180°) and falls rapidly below 20 for more oblique wave normal angles (~140°). The measured $(cB_x)/E_y$ ratio on the DE 1 satellite was about 25 and corresponds to a wave normal direction of 140°.

Detection of a Magnetospheric Duct: Low Wave Normal Angle Pulse in the Southern Hemisphere

As mentioned above, the value of the ratio $(cB_x)/E_y$ gives an indication of the wave normal angle of the wave. On the basis of ray tracing simulations (next section), for nonducted wave propagation of ground transmitter signals injected in the northern hemisphere, a large wave normal angle corresponding to a lower value of the ratio $(cB_x)/E_y$ is to be expected in the southern hemisphere. From Table 2 we found this to be the case in general except for a signal observed between 1624:57 and 1625:14 UT when rather large values of B_x and $(cB_x)/E_y$ were measured (see Figure 3a and 3d) indicating low wave normal angles (< 30°). We interpret this low wave normal angle signal to be a case of ducted propagation. To further test this assumption, the electron density data were examined. As pointed out in Figure 3d, between 1625:04 and 1625:12 there was a 3000 to 3800 electrons/cm^3 enhancement over the background electron density of 29500 electrons/cm, consistent with the duct hypothesis (other variations in electron density seen in Figure 3d are presumed to be local field aligned irregularities which are commonly present in the ionosphere). Further, the equatorial gyrofrequency corresponding to L =2.85 is 34.4 kHz. Thus the 15 kHz Khabarovsk signal is well below the half gyrofrequency cutoff of $f_{Heq}/2$ = 17.2 kHz for ducted propagation [*Helliwell*, 1965].

We note here that the main difference between our measurements and previous ones is that we have for the first time provided simultaneous measurements of both wave normal direction and of electron density at high resolution inside a duct. We also provide for the first time in situ measurents of the electric and magnetic fields of a ground transmitter signal inside a duct. Previous detection of ducts was based on either measurements of whistler dispersion [*Smith and Angerami*, 1968; *Angerami*, 1970; *Scarf and Chappell*, 1973; *Carpenter et al.*, 1981] or enhancements of whistler mode hiss correlated with density enhancements [*Koons*, 1989].

Significant parameters of the duct and the ducted signals as estimated from Figure 3d are noted below:

1. The center of the duct identified in the lower panel of Figure 3d was located at L = 2.94 (λ_m = 50.9°) and ϕ_g = 144.34°. The magnetic footprint of the duct was located at about 2000 km from the Khabarovsk transmitter. The L shell thickness of the duct was 0.06 and corresponds to a duct cross section of 55 km at 981 km altitude and 367 km at the geomagnetic equator. The density enhancement was 10-13% over the background electron density

of 29500 electrons/cm. Only a lower limit of $\Delta\phi \geq 0.2^\circ$ can be placed on the longitudinal extent of the duct, consistent with the 3°-4° of width in longitude estimated by *Angerami* [1970]. The density within the duct shows fine structure over a 5-10 km scale.

The measured duct thickness of 367 km at the equator and the density enhancement of 10-13% agree well with those measured by previous authors: ~400 km near $L = 3$ by *Smith and Angerami* [1968], 223-430 km and 6-22% for $L = 4.1 - 4.7$ by *Angerami*, [1970] 68-850 km and 10-40 % for $L = 3.1 - 3.5$ by *Scarf and Chappell* [1973], 630-1260 km and $\leq$ 30% between $L = 4$ and $L = 5$ by *Carpenter et al.* [1981], and ~ 500 km and ~ 40% by *Koons* [1989].

The efficiency of signal coupling between the Earth-ionosphere waveguide and magnetospheric ducts is of importance to studies of VLF propagation and wave amplification in the magnetosphere. This coupling is critically dependent on the duct end points in the ionosphere [*Bernhardt and Park*, 1977]. Our study indicates that duct end points can extend down to at least ~980 km at ~ 0130 LT in the southern hemisphere during austral winter. This result is consistent with theoretical studies of *Bernhardt and Park* [1977], who predict duct end point as low as 300 km at night during winter and equinoxes.

2. The ducted signals (see Table 2) were observed over an L shell range of 0.13, about twice the L shell width of the duct. This could be the result of ducted signals leaking from the duct as previously noted in both experimental and theoretical works [*Angerami*, 1970; *Strangeways and Rycroft*, 1980; *Strangeways*, 1982]. The peak electric and magnetic field were detected inside the duct near the duct center. Both the peak electric (> 520 μV/m) and magnetic field (36 pT) intensities of the ducted signals were comparable to those observed for the nonducted signals over the transmitter in the northern hemisphere, but were about 20 dB higher than those of the nonducted signals observed in the southern hemisphere in the vicinity of the duct. Inside the duct electric and magnetic field intensities show a fine structure, consistent with recent reports of whistler fine structure by *Hamar et al.* [1990, 1992].

It has been pointed out that the strongest wave particle interactions for ducted wave takes place near the magnetic equator [*Helliwell*, 1967]. Further, the value of the wave magnetic field determines the character of the wave-particle interactions. The small signal theory of *Helliwell* [1988] assumes the magnetic field inside the duct at the equator to be $\leq$ 1 pT, whereas large signal theories [*Nunn*, 1984; *Molvig*, 1986], involving trapping of electrons in the wave magnetic field, requires an equatorial input field of the order of 5 pT or higher. It is therefore useful to calculate the equatorial electric and magnetic fields inside a duct from those measured at higher latitudes. To this end, it is necessary (1) to calculate the defocusing losses due to the increase in the duct cross section with decreasing latitude and (2) to take into account the impedance transformation due to the change in wave refractive index. Assuming a dipole magnetic field, the cross section of a duct centered at a given L shell value (L) as a function of geomagnetic latitude (λ_m) is given by

$$A(L, \lambda_m) = \frac{R_E^2 L \cos^6 \lambda_m \Delta L \Delta\phi_m}{\sqrt{1 + 3\sin^2 \lambda_m}} \tag{2}$$

where R_E is the Earth's radius, and ΔL and $\Delta\phi_m$ are the L shell and longitudinal widths of the duct. For propagation along the geomagnetic field, the power (P) carried by the wave is related to the wave electric (E) and magnetic (B) fields as follows:

$$P = \frac{\mu E^2}{377} = \frac{377 B^2}{\mu} \tag{3}$$

where μ is the whistler mode refractive index for parallel propagation. The value of μ depends on the local electron density N_e and the geomagnetic field $\mathbf{B}_0$ [*Helliwell*, 1965].

Using (2) and (3) and using the measured duct parameters, we obtain

$$B(\lambda_m = 0^\circ) = 0.33 B(\lambda_m = 50.9^\circ) \tag{4a}$$

$$E(\lambda_m = 0^\circ) = 0.11 E(\lambda_m = 50.9^\circ) \tag{4b}$$

This gives a peak magnetic field of ~ 12 pT and a peak electric field of ~ 57μV/m at the equator, sufficient to lead to wave growth by either of the mechanisms noted above. With the narrow-band measurements on COSMOS 1908 satellite, it is difficult to know if the ducted signals observed in the southern hemisphere underwent amplification in near equatorial regions due to wave particle interactions. The high values of electric and magnetic field near the equator are probably the result of the high (800 kW) radiated power of the Khabarovsk transmitter. For a transmitter such as the experimental system at Siple, Antarctica [*Helliwell*, 1988] with only 1-2 kW of radiated power, we would expect the magnetic and the electric fields inside a duct to be substantially lower. A detailed calculation of expected Siple transmitter intensities based on the results presented here are beyond the scope of this paper.

Ray Tracing Simulations

Ray tracing simulations were carried out using the Stanford VLF ray tracing program [*Inan and Bell*, 1977], which uses a diffusive equilibrium density model inside the plasmasphere and a r^{-n} dependence outside the plasmapause. A centered dipole model is assumed for the magnetic field. In our simulations, the density at 1000 km in the ionosphere was chosen to be consistent with the electron density measurements on COSMOS 1809, and the plasmapause location was estimated to be $L = 3.3$ using an empirical formula given by *Carpenter and Park* [1973]. Figure 7 shows the equatorial electron density profile used in the ray tracing simulations and Figures 8a and 8b show typical ray paths and the wave normal directions along the ray paths for 11.9- and 15.0-kHz signals respectively. Initial rays were injected with vertical wave normal directions at 500 km altitude and over a range of latitudes near that of the Khabarovsk and Alpha transmitters. Figures 8a and 8b also show the trajectory of the DE 1 satellite during the period of observations. The general conclusions from the ray tracing simulations are as follows:

1. Waves injected over a range (20°–60°) of latitude in the northern hemisphere reach the southern hemisphere (at ~1000 km altitude) at locations approximately conjugate to the injection region in the northern hemisphere. Thus a satellite such as COSMOS 1809 following a polar trajectory at a fixed altitude of ~1000 km would detect waves when it is above the transmitter and also when it is in the conjugate region. No detection of waves is expected near the equatorial region. This general picture is consistent with COSMOS 1809 observations of Khabarovsk transmitter signals (Figure 3a) and with other work such as from OGO 4 and FR 1 satellites [*Scarabucci*, 1969; *Cerisier*, 1973]. However, we note that the focusing of rays in latitude in the southern hemisphere predicted by raytracing simulations is not observed in the data. The latitude ranges over which nonducted signals were observed in the northern and southern hemispheres are comparable (Table 2).

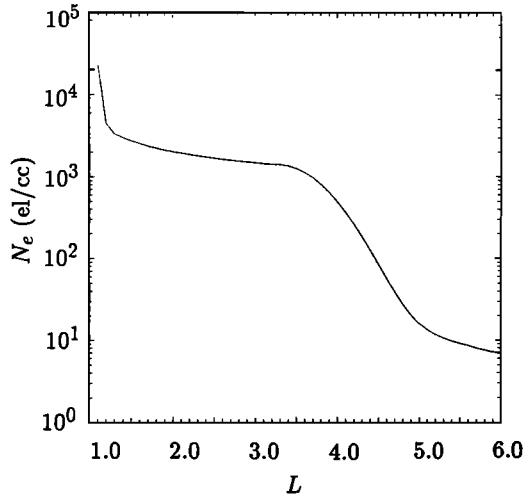

Figure 7. Equatorial electron density profile used in the ray tracing simulations.

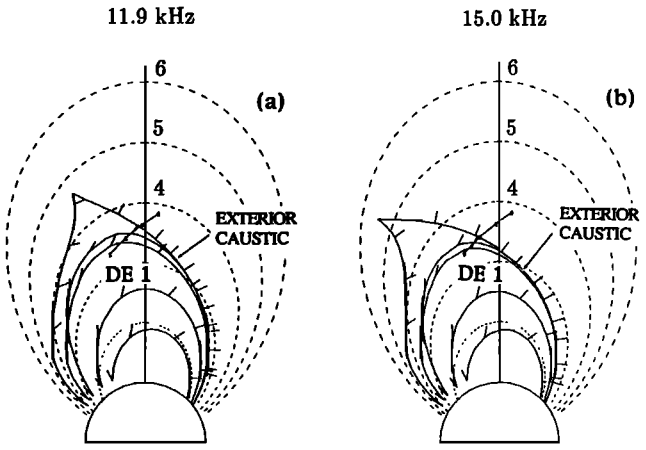

Figure 8. (a) Ray tracing simulations of 11.9-kHz Alpha transmitter signals. Initial rays were injected with vertical wave normal directions at 500 km altitude and over a range of latitudes near that of the Khabarovsk and Alpha transmitters. The L shell value and the invariant latitude of the magnetic field line at 500 km altitude directly over the Khabarovsk transmitter location are 1.73° and 40.5°, respectively. (b) Ray tracing simulations of 15.0-kHz Khabarovsk transmitter signals.

2. The predicted group delay of ~1.1 s for 15-kHz signal propagation to DE 1 altitudes compares well with the measured time delay of 1.2-1.3 s.

3. The large ratio of the peak electric and magnetic field intensities observed on the COSMOS 1809 (~500 μV/m) and DE 1 (a few microvolts per meter) satellites can be explained in terms of (1) defocusing resulting from the spreading of the rays from low altitudes (COSMOS 1809 altitude) to high altitudes (DE 1 altitude), and (2) large separation in longitude of the DE 1 satellite from the transmitter location compared to that of the COSMOS 1809 satellite.

4. The ray tracing simulations predict low wave normal directions (160-170°) (corresponding to higher $(cB_x)/E$ ratio) above the transmitter location and large wave normal directions (~90°) (corresponding to lower $(cB_x)/E$ ratios) in the conjugate region, consistent with the observations noted in Table 2. For the wave observations of the DE 1 satellite a wave normal direction of 145°-150° obtained from ray tracing agrees well with that (140°) obtained from the observed $(cB_x)/E$ ratio.

5. Figures 8a and 8b show spatial cutoffs, that is, a region in the magnetosphere that is not accessible to waves injected from the ground and propagating in the nonducted mode. The spatial cutoff corresponds to the intersection of the caustic surface with the magnetic meridional plane. Comparing Figures 8a and 8b, we note that at a given latitude, the L shell value of the spatial cutoff is a decreasing function of frequency, a result consistent with the observations displayed in Figures 4 and 5 and Table 3. The locations of the cutoffs determined from the raytracing simulations show good agreement with the measurements.

6. Wave normal directions near the caustic surface are typically within 1°-2° of the local resonance cone.

Thus we conclude that raytracing simulations support our interpretations of the available data.

Summary and Discussion

We have presented observations of Khabarovsk transmitter signals on the DE 1 and COSMOS 1809 satellites during a 9-day period in August 1989. The linear wave receiver (LWR) on the DE 1 satellite recorded wideband VLF wave data in a 10-16 kHz frequency band. On 7 out of 9 days, Khabarovsk signals were detected by LWR on the DE 1 satellite. In addition, DE 1 also detected signals from the Alpha transmitter in Russia and the Omega transmitter in Australia. Natural VLF emissions such as hiss, chorus, whistlers, and impulsive wideband signals were also observed. On 2 days, August 23 and 27, 1989, observations of Khabarovsk signals were simultaneously available at high altitude (15,000 km) on the DE 1 satellite and at low altitude (1000 km) on the COSMOS 1809 satellite. The most important results of this study using data from these 2 days are (1) confirmation of 10 – 100 km scale ionospheric density gradients as the cause of direct multiple path propagation; (2) first detection of an exterior caustic surface in the magnetosphere for VLF nonducted waves injected from the ground, involving measurements of both electric and magnetic fields across the caustic surface; (3) first direct detection of ducted signal propagation on a satellite and determination of duct parameters. Two-dimensional ray tracing simulations were performed to investigate the nonducted whistler mode propagation of Khabarovsk (15 kHz) and Alpha (11.9 kHz) signals from the transmitter locations to the DE 1 and COSMOS 1809 satellites. The results of the ray tracing simulations confirmed our interpretation of the observations.

Our results have direct implications for the question of accessibility of waves injected from the ground to various regions of the ionosphere and the magnetosphere. Particularly, using the results presented here, it is possible to estimate the wave levels as a function of frequency present in the ionosphere and magnetosphere due to waves injected from various navigational and communication transmitters and from lightning discharges. The latter are believed to play an important role in precipitating energetic electrons [*Carpenter et al*, 1984; *Inan et al.*, 1990] and generation of plasmaspheric hiss [*Sonwalkar and Inan*, 1989; *Draganov et al.*, 1992, 1993]. The detailed measurements of the electric and magnetic field on both the illuminated and dark sides of the caustic, along with wave normal measurements, can also be used to verify any future theories of caustic surfaces in an anisotropic magnetoplasma. Using the equatorial values of electric and magnetic field inside a duct and knowing the parameters of the Khabarovsk transmitter signals, it should be possible to estimate electric and magnetic field values inside a duct due to Siple Station transmitter signals. This calculation may provide critical measurements needed to differentiate between the small signal and large signal theories of wave-particle interactions [*Helliwell*, 1988; *Nunn*, 1984; *Molvig*, 1986].

Acknowledgments. We thank D. L. Carpenter, M. Walt, and T. A. Mielki for many useful comments on the manuscript. The spectrograms were produced by J. Yarborough. This research was sponsored by the National Aeronautics and Space Administration under contracts NAGS-476 and NAG5-1549.

The Editor thanks M. Parrot and G. Tarcsai for their assistance in evaluating this paper.

References

Angerami, J. J., Whistler duct properties deduced from VLF observations made with the OGO-3 satellite near the magnetic equator, *J. Geophys. Res., 75*, 6115, 1970.

Bell, T. F., and H. D. Ngo, Electrostatic waves stimulated by coherent VLF signals propagating in and ear the inner radiation belt, *J. Geophys. Res., 93*, 2599, 1988.

Bell, T. F., U. S. Inan, and R. A. Helliwell, Conducted coherent VLF waves and associated triggered emissions observed on the ISEE-1 satellite, *J. Geophys. Res., 86*, 4649, 1981.

Bell, T. F., R. A. Helliwell, and M. K. Hudson, Lower hybrid waves excited through linear mode coupling and the heating of ions in the auroral and subauroral magnetosphere, *J. Geophys. Res., 96*, 11,379, 1991.

Bernhardt, P. A., and C. G. Park, Protonospheric-ionospheric modeling of VLF ducts, *J. Geophys. Res., 82*, 5222, 1977.

Budden, K. G., *The Propagation of Radio Waves*, Cambridge University Press, New York, 1985.

Burgess, W. C., and U. S. Inan, The role of ducted whistlers in the precipitation loss and equilibrium flux of radiation belt electrons, *J. Geophys. Res., 98*, 15,643, 1993.

Burtis, W. J., and R. A. Helliwell, Magnetospheric chorus: Occurrence pattern and normalized frequency, *Planet. Space Sci., 24*, 1007, 1976.

Carpenter, D. L., and C. G. Park, On what ionospheric workers should know about the plasmapause-plasmasphere, *Rev. Geophys. Space Phys., 11*, 133, 1973.

Carpenter, D. L., R. R. Anderson, T. F. Bell and T. R. Miller, A comparison of equatorial electron densities measured by whistlers and by a satellite radio technique, *Geophys. Res. Lett., 8*(10), 1107, 1981.

Carpenter, D. L., U. S. Inan, M. L. Trimpi, R. A. Helliwell, and J. P. Katsufrakis, Perturbations of subionospheric LF and MF signals due to whistler-induced electron precipitation bursts, *J. Geophys. Res., 89*, 9857, 1984.

Cerisier, J. C., A theoretical and experimental study of non-ducted VLF waves after propagating through the magnetosphere, *J. Atmos. Terr. Phys., 35*, 77, 1973.

Dantas, N. H., 0G0-4 Satellite observations of whistler-mode propagation effects associated with countries in the magnetosphere, *Tech. Rep., 3469-1*, Stanford Electron. Lab., Stanford, Calif., 1972.

Draganov, A. B., U. S. Inan, V. S. Sonwalkar, and T. F. Bell, Magnetospherically reflected whistlers as a source of plasmaspheric hiss, *Geophys. Res. Lett., 19*, 233, 1992.

Draganov, A. B., U. S. Inan, V. S. Sonwalkar, and T. F. Bell, Whistlers and plasmaspheric hiss: Wave directions and three dimensional propagation, *J. Geophys. Res., 98*, 11,401, 1993.

Dunckel, N., and R. A. Helliwell, Spacecraft observations of man-made whistler-mode signals near the electron gyrofrequency, *Radio Sci., 12*(5), 821, 1977.

Edgar, B. C., The upper and lower frequency cutoffs of magnetospherically reflected whistlers, *J. Geophys. Res., 81*, 205, 1976.

Gurnett, D. A., S. D. Shawhan, and R. R. Shaw, Auroral hiss, *Z* mode radiation, and auroral kilometric radiation in the polar magnetosphere: DE1 observations, *J. Geophys. Res., 88*, 329, 1983.

Hamar, D., Gy. Tarcsai, J. Lientenberger, A. J. Smith, and K. H. Yearby, Fine structure of whistlers recorded digitally at Halley, Antarctica, *J. Atmos. Terr. Phys., 52*, 801, 1990.

Hamar, D., Cs. Ferencz, J. Lichtenberger, Gy. Tarcsai, A. J. Smith, and K. H. Yearby, Trace splitting of whistlers: A signature of fine structure or mode splitting in magnetospheric ducts? *Radio Sci., 27*, 341, 1992.

Hayakawa, M., M. Parrot, and F. Lefeuvre, The wave normals of ELF hiss emissions observed on board GEOS 1 at the equatorial and off-equatorial regions of the plasmasphere, *J. Geophys. Res., 91*, 7989, 1986.

Helliwell, R. A., *Whistlers and Related Ionospheric Phenomena*, Stanford University Press, Stanford, Calif., 1965.

Helliwell, R. A., A theory of discrete VLF emissions from the magnetosphere, *J. Geophys. Res., 72*, 4773, 1967.

Helliwell, R. A., VLF wave stimulation experiments in the magnetosphere from Simple Station, Antarctica, *Rev. Geophys., 26*, 551, 1988.

Helliwell, R. A., J. P. Katsufrakis, and M. L. Trimpi, Whistler-induced amplitude perturbations in VLF propagation, *J. Geophys. Res., 78*, 4679, 1973.

Inan, U. S., and T. F. Bell, The plasmapause as a VLF wave guide, *J. Geophys. Res., 82*, 2819, 1977.

Inan, U. S., F. A. Knifsend, and J. Oh, Subionospheric VLF "imaging" of lightning-induced electron precipitation from the magnetosphere, *J. Geophys. Res., 95*, 17,217, 1990.

Jasna, D., U. S. Inan, and T.F. Bell, Equatorial gyroresonance between electrons and magnetospherically reflected whistlers, *Geophys. Res. Lett., 17*, 1865, 1990.

Jasna D., U. S. Inan, and T. F. Bell, Precipitation of suprathermal (100 eV) electrons by oblique whistler waves, *Geophys. Res. Lett., 19*, 1639, 1992.

Koons, H. C., Observations of large-amplitude, whistler mode wave ducts in the outer plasmasphere, *J. Geophys. Res., 94*, 15,393, 1989.

Lefeuvre, F., M. Parrot, L. R. O. Storey, and R. R. Anderson, Wave distribution functions for plasmaspheric hiss observed on board ISEE 1, *Tech. Note LPCE/6*, Lab. de Phys. et Chim. de l'Environ, Orleans, France, 1983.

Maggs, J. E., Coherent generation of VLF hiss, *J. Geophys. Res., 81*, 1707, 1976.

Molvig, K., G. Hilfer, and J. Myczkowski, Self-consistent theory of triggered whistler emissions, *Eos, Trans. AGU, 67*(44), 1166, 1986.

Neubert, T., E. Ungstrup, and A. Bahnsen, Observations on the GEOS 1 satellite of whistler mode signals transmitted by the omega navigation system transmitter in northern Norway, *J. Geophys. Res., 88*, 4015, 1983.

Nunn, D., The quasi static theory of triggered VLF emissions. *Planet. Space Sci., 32*, 325, 1984.

Ondoh, T., Y. Nakamura, S. Watanabe, K. Aikyo, M. Sato, and F. Sawada, Impulsive plasma waves observed by the DE 1 in the nightside outer radiation zone, *J. Geophys. Res., 94*, 3779, 1989.

Rastani, K., U. S. Inan, and R. A. Helliwell, DE-1 observations of Siple transmitter signals and associated sidebands, *J. Geophys. Res., 90*, 4128, 1985.

Rosenberg, T. J., R. A. Helliwell, and J. P. Katsufrakis, Electron precipitation associated with discrete very-low-frequency emissions, *J. Geophys. Res., 76*, 8445, 1971.

Scarabucci, R. R., Interpretation of VLF signals observed on the OGO-4 satellite, *Tech. Rep. 3418-2*, Stanford Electron. Lab., Stanford, Calif., 1969.

Scarf, F. L., and C. R. Chappell, An association of magnetospheric whistler dispersion characteristics with changes in local plasma density, *J. Geophys. Res., 78*, 1597, 1973.

Shawhan, S. D., D. A. Gurnett, D. L. Odem, R. A. Helliwell, and C. G. Park, The plasma wave and quasi-static electric field instrument (PWI) for Dynamic Explorer-A, *Space Sci. Instrum., 5*, 535, 1981.

Smith, R. L., and J. J. Angerami, Magnetospheric properties deduced from OGO 1 observations of ducted and non-ducted whistlers, *J. Geophys. Res., 73*, 1, 1968.

Smith, R. L., R. A. Helliwell, and I. W. Yabroff, A theory of trapping of whistlers in field-aligned columns of enhanced ionization, *J. Geophys. Res., 65*, 815, 1960.

Sonwalkar, V. S., *New Signal Analysis Techniques and Their Applications to Space Physics*, Ph.D. thesis, Stanford Univ., Stanford, Calif., June 1986.

Sonwalkar, V. S., and U. S. Inan, Measurements of Siple transmitter on the DE 1 satellite: Wave normal direction and antenna effective length, *J. Geophys. Res., 91*, 154, 1986.

Sonwalkar, V. S. and U. S. Inan, Wave normal direction and spectral properties of whistler-mode hiss observed on the DE-1 satellite, *J. Geophys. Res., 93*, 7493, 1988.

Sonwalkar, V. S., and U. S. Inan, Lightning as an embryonic source of VLF hiss, *J. Geophys. Res., 94*, 6986, 1989.

Sonwalkar, V. S., T. F. Bell, R. A. Helliwell, and U. S. Inan, Direct multiple path magnetospheric propagation: a fundamental property of nonducted VLF waves, *J. Geophys. Res., 89*, 2823, 1984.

Sonwalkar, V. S., R. A. Helliwell, and U. S. Inan, Wideband VLF electromagnetic busts observed on the DE 1 satellite, *Geophys. Res. Lett., 17*, 1861, 1990.

Storey, L. R. O., F. Lefeuvre, M. Parrot, L. Cairo, and R. R. Anderson, Initial survey of the wave distribution functions for plasmaspheric hiss observed by ISEE 1, *J. Geophys. Res., 96*, 19,469, 1991.

Strangeways, H. J., The effect of multi-duct structure on whistler-mode wave propagation, *J. Atmos. Terr. Phys., 44*, 901, 1982.

Strangeways, H. J. and M. J. Rycroft, Trapping of whistler-mode waves through the side of ducts, *J. Atmos. Terr. Phys., 42*, 983, 1980.

Thorne, R. M., E. J. Smith, R. K. Burton, and R. E. Holzer, Plasmaspheric hiss, *J. Geophys. Res., 78*, 1581, 1973.

Voss, H. D., W. L. Imhof, J. Mobilia, E. E. Gaines, M. Walt, U. S. Inan, R. A. Helliwell, D. L. Carpenter, J. P. Katsufrakis, H. C. Chang, Lightning induced electron precipitation, *Nature, 312*,740, 1984.

T. F. Bell, R. A. Helliwell, U. S. Inan, and V. S. Sonwalkar, STAR Laboratory, Stanford University, Stanford, CA 94305-4055. (e-mail: Internet bell@nova.stanford.edu; Internet helliwell@star.stanford.edu; Internet inan@nova.stanford.edu; Internet vss@star.stanford.edu;)

V. M. Chmyrev, O. Ya. Ovcharenko, V. Selegej, and Ya. P. Sobolev, Institute of Terrestrial Magnetism, Ionosphere and Radiowave Propagation, USSR Academy of Sciences, Troitsk, Moscow Region, Russia.

(Received January 24, 1994; revised March 28, 1994; accepted March 30, 1994.)